Hydrodynamics of Cocurrent Gas-Liquid-Solid Semifluidization with a Liquid as the Continuous Phase

The hydrodynamic behavior of a cocurrent gas-liquid-solid semifluidized bed was investigated. A separate investigation was performed on a packed bed and a fluidized bed under gas-liquid flow conditions similar to that for the semifluidized bed. Parameters of the semifluidized bed under extensive study include pressure drop, gas holdup, onset liquid velocity for semifluidization, and the height of the packed bed section and the fluidized section. The pressure drop of the semi-fluidized bed obtained experimentally was compared favorably with that predicted by the model equations.

SONG-HSING CHERN, LIANG-SHIH FAN, and K. MUROYAMA

Department of Chemical Engineering
The Ohio State University
Columbus, OH 43210

SCOPE

A semifluidized bed is formed when a mass of fluidized particles is compressed by fluids with a porous retaining grid. This gives rise to the creation of a fluidized bed and a fixed bed in series within a single containing vessel. Studies of semifluidization have been limited to the gas-solid or liquid-solid systems (e.g., Fan and Wen, 1961). Only until recently has semifluidization in the gas-liquid-solid system been explored by Chern et al. (1981). Their investigation was concerned with the hydrodynamic behavior of inverse semifluidization in which countercurrent flow of a gas and a liquid takes place in a bed of particles with the density lower than that of a liquid.

In this study, hydrodynamic behavior of semifluidization in which cocurrent flow of a gas and a liquid takes place in a bed of particles with the density higher than that of a liquid was investigated. Various parameters under extensive analysis include pressure drop, gas holdup, onset liquid velocity for semifluidization, and the height of the packed section and fluidized section. Separate experiments on the packed bed were performed to simulate the flow behavior in the packed section of the semifluidized bed.

CONCLUSIONS AND SIGNIFICANCE

The separated flow concept was adopted satisfactorily in this study to describe the pressure drop behavior in the cocurrent gas-liquid upward flow in a packed bed. The friction factor between the liquid and the solid in the packed bed was defined and empirically correlated as a function of the liquid Reynolds number. The gas holdup in the packed bed was shown to increase with the decrease of the liquid velocity and the increase of the gas velocity.

The simplified generalized wake model, more specifically, the solid-free wake model, was utilized to account for the bed expansion behavior in the gas-liquid-solid fluidized bed. With modification, Nicklin's theory for the two-phase bubble flow and the slug flow elucidates well the gas holdup in the dispersed bubble flow regime and the slug flow regime for the gas-liquid-solid fluidized bed.

Based on the bed expansion characteristics of the fluidized bed, the onset liquid velocity for gas-liquid-solid semifluidization was established. The height of the packed section in the semifluidized bed was found to be predictable directly from a simple material balance equation for the solid particles in the bed. Following the model equations developed in this study the pressure drop in the semifluidized bed which is the sum of the pressure drop in the packed section and that in the fluidized section was reasonably predicted.

INTRODUCTION

The phenomenon of semifluidization was first reported by Fan et al. (1959) in the subject which was concerned with the mass transfer in the semifluidized bed in the liquid-solid systems. A semifluidized bed which is characterized by a fluidized bed and a fixed bed in series within a single containing vessel is formed when a mass of fluidized particles is compressed by fluids with a porous-retaining grid. The internal structure of a semifluidized bed can easily be altered to create an optimal operating configuration. This unique feature allows the semifluidized bed to be utilized for a wide range of physical, chemical and biochemical applications (e.g., Babu Rao and Doraiswamy, 1970; Chementator, 1972; Fan and Wen, 1979).

Studies of semifluidization have been mainly limited to the gas-solid or liquid-solid systems (Fan and Wen, 1961; Wen et al., 1963; Babu Rao and Doraiswamy, 1970; Roy and Gupta, 1974; Roy and Chandra, 1976; Roy and Sarma, 1978). Little information, however, is available on semifluidization in the gas-liquid-solid systems (Chern et al., 1981). Chern et al. (1981) investigated the hydrodynamic behavior of the inverse gas-liquid-solid semifluidized bed where a liquid is the continuous phase. A mathematical model was proposed to account for the pressure drop in the inverse gas-liquid-solid semifluidized bed.

In this paper, hydrodynamic characteristics, specifically the pressure drop and gas holdup of a cocurrent gas-liquid-solid semifluidized bed, are studied. The bed expansion of the cocurrent gas-liquid-solid fluidization is also investigated in conjunction with the study of the onset liquid velocity for semifluidization and the height of the packed section of the semifluidized bed. Furthermore, experiments are carried out to examine the pressure drop and gas holdup in the packed bed with cocurrent upward flow of the gas

Correspondence concerning this paper should be addressed to L.-S. Fan.
K. Muroyama is on leave from the Department of Environmental Chemistry and Technology, Tottori University, Tottori 680, Japan.

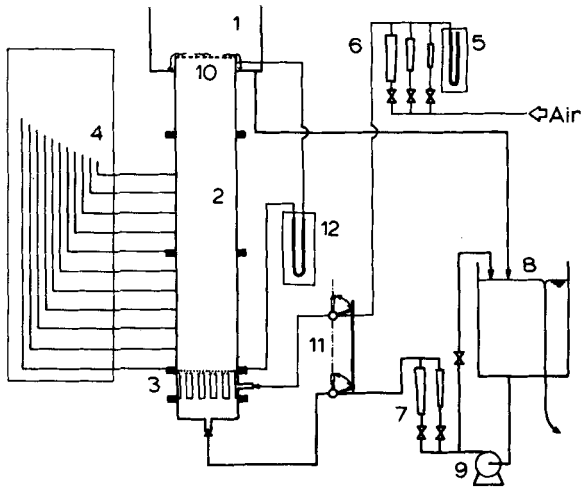

1 Gas-Liquid Disengagement Section
2 Test Section
3 Gas-Liquid Distributor Section
4 Manometers
5 Pressure Gauge
6,7 Rotameters
8 Liquid Reservoir
9 Liquid Pump
10 Retaining Grid
11 Quick-Closing Valves
12 Mercury Differential Manometer

Figure 1. Experimental apparatus for the study of hydrodynamic characteristics of a cocurrent gas-liquid-solid semifluidized bed.

and the liquid. These experiments simulate the flow behavior in the packed section of the semifluidized bed. Utilizing the model of the pressure drop for the packed bed and that for the fluidized bed, the prediction of the pressure drop in the semifluidized bed is demonstrated.

EXPERIMENTAL

The schematic diagram of the experimental apparatus is shown in Figure 1. The vertical Plexiglas column in Figure 1 is of 76.2 mm ID with a maximum height of 2.730 m. The column consists of three sections, namely, the gas-liquid disengagement section, test section, and gas-liquid distributor section. The gas-liquid distributor is located at the bottom of the test section and is designed in such a manner that uniform distributions of the liquid and gas can be maintained in the column. Details of the distributor design are given by Fan et al. (1982).

Water and air are used in the experiments. The gas-liquid flow is cocurrent and upward. Rotameters are used for measurement of the gas and liquid flow rates which vary from 0 to 25.67 cm/s and from 2.184 to 16.90 cm/s, respectively. Pressure taps are connected to water manometers or mercury manometers for measurement of the static pressure drop along the column.

A separate experiment is performed to examine the hydrodynamic behavior of the packed bed with the cocurrent upward flow of the gas and the liquid in this study. This experiment is intended to simulate the hydrodynamic behavior in the packed section of the semifluidized bed. The height of the packed bed is 60.69 cm. The static pressure gradients are measured by a manometer at two points located at 10.2 cm from the bottom and the top of the packed bed. The quick-closing valve method is used to determine the gas holdup in the packed bed. The method involves the simultaneous shutoff of the valves connected to the liquid and gas inlets. The trapped liquid is then drained and measured. With the height of the packed bed known, the gas holdup can be calculated. Three different particles referred to as Particles I–III are used in the experiments. The physical properties of these particles are summarized in Table 1.

PACKED BED BEHAVIOR

Pressure Drop

The hydrodynamic behavior of the cocurrent gas-liquid upward flow in the packed bed is very complex. Three different flow modes

TABLE 1. PHYSICAL PROPERTIES OF PARTICLES

Particle	Material	Shape	ρ_s (g/cm³)	$\phi_s d_p$ (cm)	Richardson-Zaki Eq.'s Parameters Experimentally Obtained U_i (cm/s)	$n(-)$
I	Glass	Sphere	2.520	0.3	24.78	2.434
II	Glass	Sphere	2.201	0.6	34.16	2.313
III	Poly-vinyl Chloride	Cylinder*	1.470	0.3	18.42	2.340

* The length is equivalent to the diameter.

have been observed in the packed bed, namely the gas continuous flow, the pulse flow and the dispersed bubble flow (Turpin and Huntington, 1967; Sato et al., 1974). The packed bed under which the present pressure drop experiments are conducted operates mainly in the pulse flow mode. A simplified two-phase flow model, specifically the separated flow model (Wallis, 1969) which was extended by Matsuura et al. (1977) to account for the pressure drop behavior of cocurrent downward gas-liquid flow in a packed bed, is adopted with modification in this study.

The model considers that gas and liquid flows are one-dimensional and the solid particles can be completely wetted by the liquid and, thus, there is no direct contact between the gas and solid. Under such a condition, the system is viewed to be represented by three distinct phases, i.e., the gas phase in the core area, the solid phase in the wall area, and the liquid phase in the annular area.

Assuming the momentum transfer due to acceleration of each phase is negligible, the momentum balance for the liquid and gas phases in the packed bed under the steady-state conditions can be expressed respectively, by

$$\left(-\frac{dP}{dz}\right)^p = \rho_l g + \left(-\frac{dP}{dz}\right)_f^l \tag{1}$$

$$\left(-\frac{dP}{dz}\right)^p = \rho_g g + \left(-\frac{dP}{dz}\right)_f^g \tag{2}$$

where $(-dP/dz)_f^\ell$ is the frictional pressure drop in the liquid phase which consists of two components; one is contributed by the solid phase or $(-dP/dz)_f^{\ell-s}$, and the other is contributed by the gas phase or $(-dP/dz)_f^{\ell-g}$. Mathematically, it can be represented by

$$\left(-\frac{dP}{dz}\right)_f^l = \left(-\frac{dP}{dz}\right)_f^{l-s} + \left(-\frac{dP}{dz}\right)_f^{l-g} \tag{3}$$

The frictional pressure drop in the gas phase, or $(-dP/dz)_f^g$ consists of only one component, which is contributed by the liquid phase. Mathematically, it can be represented by

$$\left(-\frac{dP}{dz}\right)_f^g = \left(-\frac{dP}{dz}\right)_f^{g-l} \tag{4}$$

Since the mutual force in the interface is cancelled by each other, we have

$$\theta_l \left(-\frac{dP}{dz}\right)_f^{l-g} + \theta_g \left(-\frac{dP}{dz}\right)_f^{g-l} = 0 \tag{5}$$

where

$$\theta_l = \frac{\epsilon_l^p}{1 - \epsilon_s^p} \tag{6}$$

$$\theta_g = \frac{\epsilon_g^p}{1 - \epsilon_s^p} \tag{7}$$

Note that

$$\theta_l + \theta_g = 1 \tag{8}$$

From Eqs. 1 through 5 and 8, we obtain

$$\left(-\frac{dP}{dz}\right)^p = \theta_l \left(-\frac{dP}{dz}\right)_f^{l-s} + (\theta_l \rho_l + \theta_g \rho_g) g \tag{9}$$

or

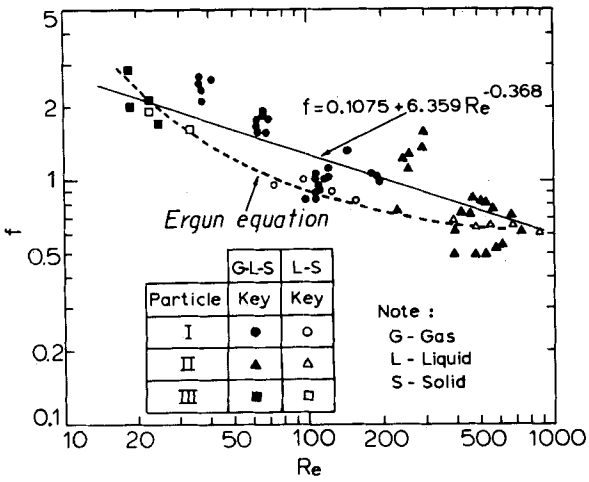

Figure 2. Variation of the friction factor f with Re.

$$\left(-\frac{dP}{dz}\right)_f^{l-s} = \frac{1}{\theta_l}\left[\left(-\frac{dP}{dz}\right)^p - (\theta_l\rho_l + \theta_g\rho_g)g\right] \tag{10}$$

Equation 9 expresses the static pressure gradient in terms of the frictional pressure gradient between the liquid and the solid and the weight per unit volume for the gas and liquid phases.

The frictional pressure drop between the liquid and the solid can be expressed by Fanning's equation as

$$\left(-\frac{dP}{dz}\right)_f^{l-s} = 4f\left(\frac{1}{D_e}\right)\left[\frac{1}{2}\rho_\ell\left(\frac{U_{\ell 0}}{\epsilon_\ell^p}\right)^2\right] \tag{11}$$

where f is the modified friction factor and D_e is the effective diameter of the channel for liquid flow. Based on the separated flow model assumption described earlier, D_e can be derived from the geometrical analysis which has the following form:

$$D_e = \frac{2(1-\epsilon_s^p)}{3\epsilon_s^p}[1 - \sqrt{\theta_g}]\phi_s d_p \tag{12}$$

where ϕ_s is the sphericity of the particle and d_p is the equivalent diameter of the particle.

The value of f is found to be a function of the liquid Reynolds number, Re, as given in Figure 2. It is seen in the figure that as Re increases, f decreases. f can be empirically correlated as a function of Re by

$$f = 0.1075 + 6.359\,Re^{-0.368} \tag{13}$$

where Re is defined as

$$Re = \frac{D_e\rho_l U_{l0}}{\mu_l\epsilon_l^p} \tag{14}$$

The agreement between Eq. 13 and experimental data for f is satisfactory.

Also shown in Figure 2 are the experimental data obtained in this work for the single-phase flow involving liquid through the packed bed. It is seen the value of f for the liquid flow in the packed bed can well be represented by Eq. 13. Note that the f vs. Re relationship described by Eq. 13 is also valid for the flow conditions under which θ_g approaches zero. A plot of f vs. Re based on the Ergun equation is also presented in the figure. It is seen that the data for the liquid flow in the packed bed fall within the range of accuracy predicted by the Ergun equation.

It is found that the static pressure gradient in the packed bed calculated from Eq. 9 using the predicted values of f and θ_g agrees reasonably well with that obtained experimentally with the average coefficient of variation of about 30%. The equation which predicts θ_g is described in the following section.

Gas Holdup

The gas holdup in the packed bed, ϵ_g^p, is empirically correlated in this study. ϵ_g^p, which is expressed in terms of θ_g defined by Eq. 7 is found to be closely correlated with $U_{\ell 0}$ and U_{g0} as given by

$$\theta_g = 0.0296(U_{l0})^{-0.350}(U_{g0})^{0.977} \tag{15}$$

Equation 15 indicates that the gas holdup increases with the decrease of the liquid velocity and the increase of the gas velocity. The average coefficient of variation for Eq. 15 is 18.2%.

FLUIDIZED BED BEHAVIOR

The solid holdup, ϵ_s^f, and the gas holdup, ϵ_g^f, in a cocurrent gas-liquid-solid fluidized bed can be calculated from the following equations (Ostergaard, 1969):

$$(-\Delta P)^f = (\epsilon_s^f\rho_s + \epsilon_l^f\rho_l + \epsilon_g^f\rho_g)Hg \tag{16}$$

$$\epsilon_s^f = W_s/(\rho_s AH) \tag{17}$$

$$\epsilon_g^f + \epsilon_l^f + \epsilon_s^f = 1 \tag{18}$$

where $(-\Delta P)^f$ and H can be determined experimentally.

Bed Expansion

The generalized wake model proposed by Bhatia and Epstein (1974) is utilized to account for the bed expansion behavior in the gas-liquid-solid fluidized bed. In the generalized wake model, three regions in the bed are considered, i.e., the bubble region, the wake region, and the liquid-solid fluidized bed region. Furthermore, the wake rises with the bubble at the bubble rising velocity. The extent of solids holdup in the wake is determined by the gas and liquid velocities and the physical properties of the particles, such as density, size, and wettability (Armstrong et al., 1976; El-Temtamy and Epstein, 1978). Based on the generalized wake model, the bed voidage, $\epsilon_g^f + \epsilon_\ell^f$, can be expressed by (Bhatia and Epstein, 1974)

$$\epsilon_g^f + \epsilon_l^f = \left[\frac{U_{l0} - U_{g0}k(1-x)}{U_i(1-\epsilon_g^f - k\epsilon_g^f)}\right]^{1/n}[1 - \epsilon_g^f(1+k-kx)] + \epsilon_g^f(1+k-kx) \tag{19}$$

where $U_{\ell 0}$ and U_{g0} are the superficial liquid and gas velocities respectively, U_i is the extrapolated superficial liquid velocity in the liquid-solid fluidized bed as the bed voidage approaches 1, n is the Richardson–Zaki index (Richardson and Zaki, 1954), k is the ratio of the volume of the wake region to that of the bubble region, $\epsilon_w^f/\epsilon_g^f$, and x is the ratio of the solids holdup in the wake region to that in the liquid-solid fluidized bed region, $\epsilon_w^f/\epsilon_{sf}^f$.

Since the particles used in this study are much larger than 1 mm in diameter, these particles would not be held in the wake region (El-Temtamy and Epstein, 1978). Thus x can be set as 0, and Eq. 19 can be simplified to

$$\epsilon_g^f + \epsilon_l^f = \left[\frac{U_{l0} - U_{g0}k}{U_i(1-\epsilon_g^f - k\epsilon_g^f)}\right]^{1/n}[1 - \epsilon_g^f(1+k)] + \epsilon_g^f(1+k) \tag{20}$$

It is evident that in order to use Eq. 20 to estimate the bed expansion k and ϵ_g^f are required to be known. The parameters, U_i and n, in the Richardson-Zaki equation are determined in separate experiments for Particle I through Particle III in the liquid-solid fluidized bed. The values of U_i and n obtained from these experiments are listed in Table 1. It is seen that these values agree reasonably well with those predicted by Richardson and Zaki (1954), i.e., n = 2.39, 2.39 and 2.39, and U_i = 27.27, 38.73 and 22.45 cm/s for Particles I, II and III, respectively. The values of U_i and n listed in Table 1 are used in the analysis of k as given in the following.

For a bed of 550 μm particles, Rigby and Capes (1970) reported that k is strongly influenced by the bubble size for a single bubble system. Furthermore, as the bubble size increases, the value of k decreases monotonically. For a multibubble system, k can be taken as an average value over the bed and can be calculated from the phase holdup data by Eq. 20. Based on the solid free wake model, correlation equations for k were proposed by several investigators

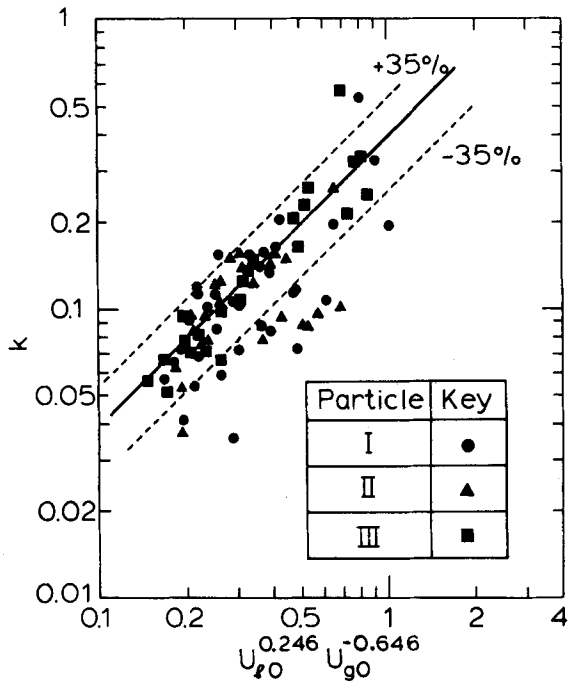

Figure 3. Correlation between k and U_{l0} and U_{g0} for the cocurrent gas-liquid-solid fluidized bed.

(Efremov and Vakrushev, 1970; Darton and Harrison, 1975; Baker et al., 1977). The value for k obtained in this study is found to decrease considerably with the increase of the gas velocity, and to increase with the increase of the liquid velocity. This variation is consistent with those reported by Darton and Harrison (1975) and Baker et al. (1977). The correlation equation of Darton and Harrison (1975), however, yields unreasonably low values of k for the range of $U_{\ell 0}/U_{g0} < 0.3$. The prediction of k by the correlation equation of Baker et al. (1977) is found to be fair.

The value of k for the present system can be empirically expressed by

$$k = 0.398 U_{l0}^{0.246} U_{g0}^{-0.646} \tag{21}$$

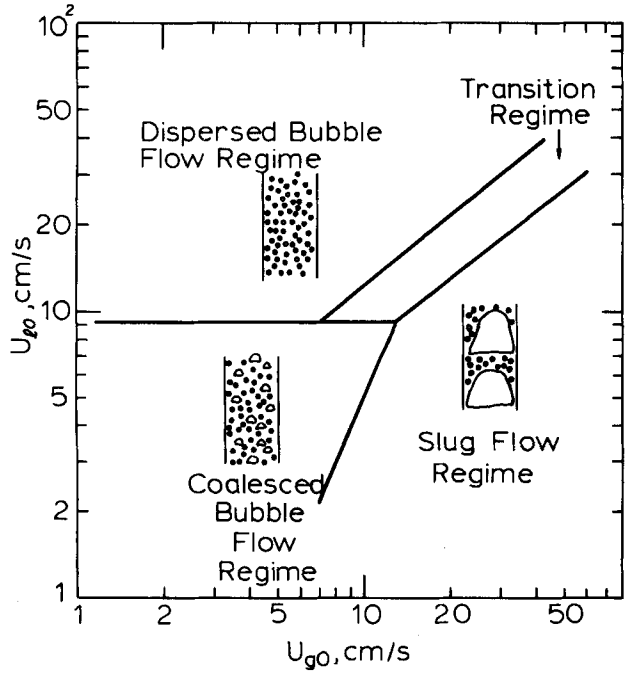

Figure 4. Flow regimes for the cocurrent gas-liquid-solid fluidized bed for particles I–III.

The accuracy of this correlation equation is shown in Figure 3.

Gas Holdup

The gas holdup in the gas-liquid-solid fluidized bed varies strongly with bubble flow properties. Depending on the gas flow rate, liquid flow rate, and physical properties of the particles, bubble flow in a gas-liquid-solid fluidized bed can be classified into three distinct regimes, namely, dispersed bubble flow regime, coalesced bubble flow regime, and slug flow regime (Muroyama et al., 1978). A flow regime map similar to that of Muroyama et al. (1978) is drawn on the U_{g0} versus $U_{\ell 0}$ coordinates as shown in Figure 4 for various particles used in this study. Note that the boundaries between the flow regimes do not vary significantly with respect to the size and shape of the particles employed.

In the dispersed bubble flow regime of the gas-liquid-solid fluidized-bed system, the bubbles are small and practically uniform in size. The increase in the gas flow rate increases the bubble frequency. In the transition regime the increase in the gas flow rate increases the bubble coalescence. However, the bubble frequency remains practically constant as the gas flow rate increases. In the slug-flow regime, the increase in the gas flow rate increases the slug frequency.

It is assumed in this study that the gas-liquid phases in the dispersed bubble flow regime and the slug flow regime of the gas-liquid-solid fluidized bed behave as a two-phase bubble column. In addition, the Nicklin theory (Nicklin, 1962) for two-phase bubble flow and slug flow can be modified to account for the gas holdup in the gas-liquid-solid fluidized bed. The gas holdup in the coalesced bubble flow regimes, however, is treated empirically due to the difficulty in accurately estimating the bubble size and size distribution in the gas-liquid-solid fluidized bed system.

Based on the Nicklin theory, the velocity of the bubbles or slugs is considered to consist of three components including the superficial liquid velocity, $U_{\ell 0}$, the superficial gas velocity, U_{g0}, and the velocity of bubbles due to buoyant force in the stagnant liquid, U_0. It can mathematically be represented by

$$\frac{U_{g0}}{\epsilon_g''} = U_{g0} + U_{l0} + U_0 \tag{22}$$

Note that U_0 varies with the bubble size and spacing and the properties of the systems.

For the slug flow, a single slug rises at a velocity of $0.35\,(gD)^{1/2}$ (Nicklin, 1962), and thus Eq. 22 applied to this flow becomes

$$\frac{U_{g0}}{\epsilon_g''} = \alpha(U_{g0} + U_{l0}) + 0.35(gD)^{1/2} \tag{23}$$

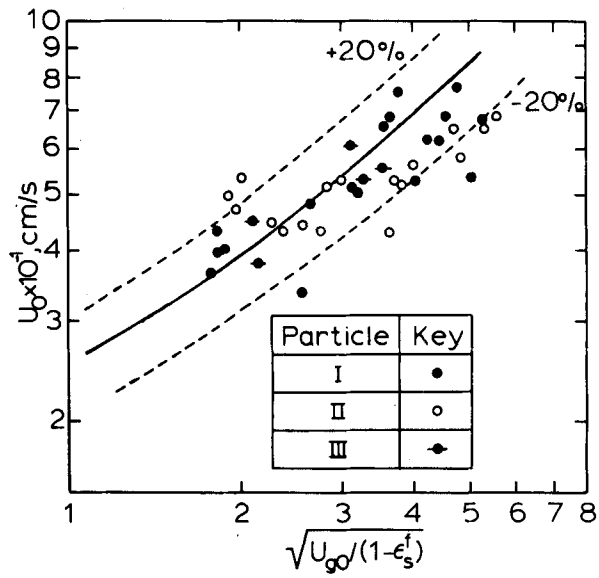

Figure 5. Correlation between U_0 and $\sqrt{U_{g0}/(1-\epsilon_s')}$ for the dispersed bubble flow regime of the cocurrent gas-liquid-solid fluidized bed.

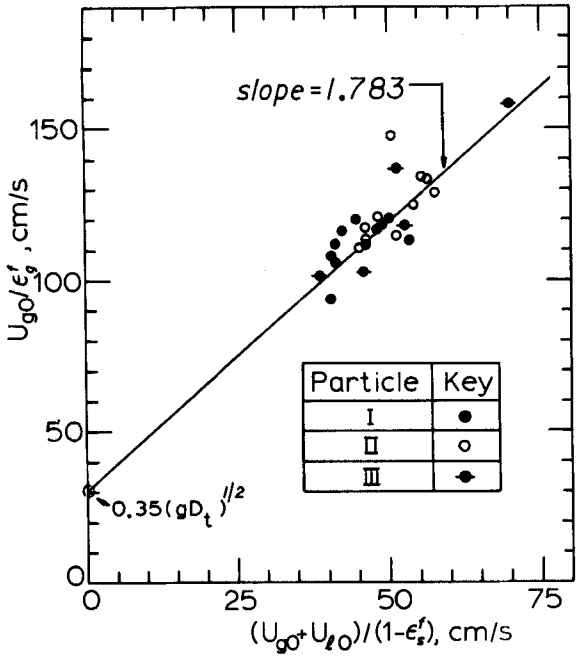

Figure 6. Gas holdup in the slug-flow regime of the cocurrent gas-liquid-solid fluidized bed.

The parameter α in Eq. 23 is introduced to account for the nonuniformity of the liquid velocity between slugs. In Nicklin's work, the value of α was found to be 1.2.

In the gas-liquid-solid fluidized bed, the gas-liquid phases in the system behave as those in a bubble column, thus, Eqs. 22 and 23 can be modified as

$$\frac{U_{g0}}{\epsilon_g^f} = \frac{U_{g0}}{1-\epsilon_s^f} + \frac{U_{l0}}{1-\epsilon_s^f} + U_0 \tag{24}$$

for the dispersed bubble flow regime

$$\frac{U_{g0}}{\epsilon_g^f} = \alpha\left(\frac{U_{g0}}{1-\epsilon_s^f} + \frac{U_{l0}}{1-\epsilon_s^f}\right) + 0.35\sqrt{gD} \tag{25}$$

for the slug-flow regime

where $U_{g0}/(1-\epsilon_s^f)$ and $U_{\ell 0}/(1-\epsilon_s^f)$ represent the superficial gas and liquid velocities based on the gas-liquid phases, respectively. Figure 5 shows that U_0 in Eq. 24 can be correlated with $U_{g0}/(1-\epsilon_s^f)$ by

$$U_0 = 10.16 + 14.88\sqrt{\frac{U_{g0}}{1-\epsilon_s^f}} \tag{26}$$

Figure 6 shows that the value of α in Eq. 25 which allows the best fit of the experimental data is 1.783.

Note that for the transition regime, the gas holdup can be approximated by the average of that calculated by Eqs. 24 and 26 for the dispersed bubble flow regime and Eq. 25 for the slug-flow regime.

In the coalesced bubble flow regime, the gas holdup is empirically obtained and correlated with $U_{\ell 0}$ and U_{g0} as shown in Figure 7 as

$$\epsilon_g^f = 0.098 U_{l0}^{-0.98} U_{g0}^{0.70} \tag{27}$$

The average coefficient of variation for this correlation is 17.3%.

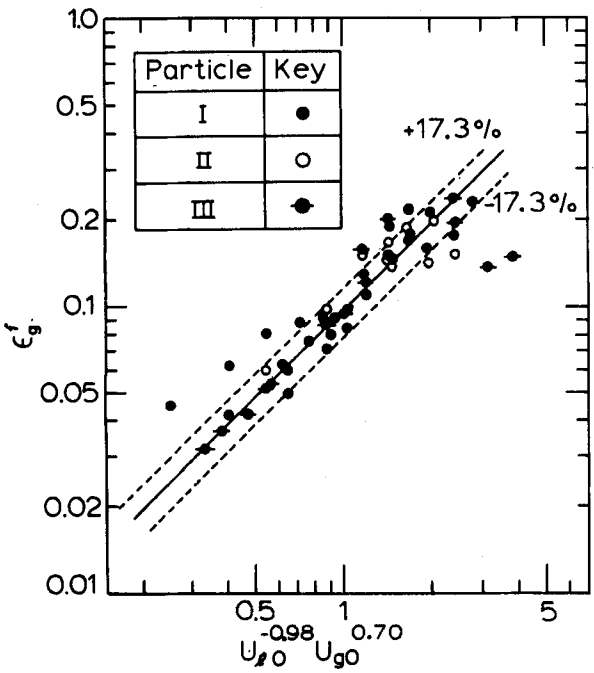

Figure 7. Gas holdup in the coalesced bubble flow regime of the cocurrent gas-liquid-solid fluidized bed.

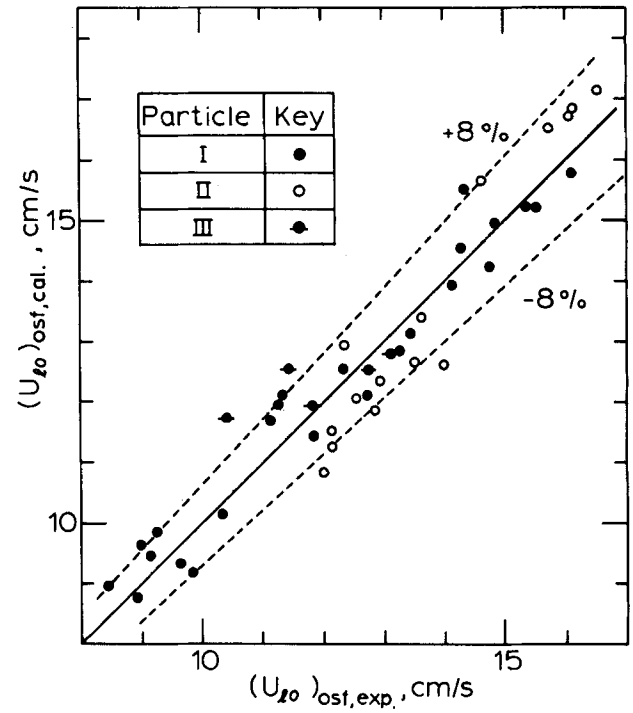

Figure 8. Comparison of the calculated and experimental values for $(U_{\ell 0})_{ost}$.

SEMIFLUIDIZED BED BEHAVIOR

The transition from fluidization to semifluidization is evident from a sharp increase of the pressure drop in the bed.

Onset Velocity for Semifluidization, $(U_{l0})_{osf}$

$(U_{\ell 0})_{osf}$ is defined as the liquid velocity at which the upper retaining grid is first packed with particles. $(U_{\ell 0})_{osf}$ can be measured directly by visualization. However, as described in the following, it can also be calculated from the extrapolation of the bed expansion relationship for the fluidized bed:

Denote the distance between the upper and lower retaining grids as H_c, and the initial weight of particles as W_s. Semifluidization would occur when the bed expands to such an extent that ϵ_s^f equals $(\epsilon_s)_{osf}$, which is defined as

$$(\epsilon_s)_{osf} = \frac{W_s}{\rho_s A H_c} \tag{28}$$

Thus, the onset liquid velocity for semifluidization decreases as the gas velocity increases.

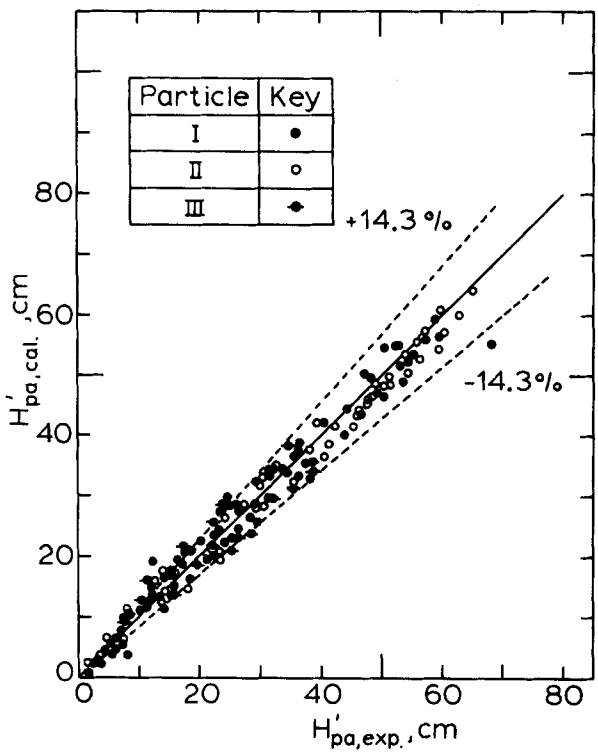

Figure 9. Comparison of the calculated and experimental values of H'_{pa} in the semifluidized bed.

From Eq. 20 with the substitution of $(\epsilon_s)_{osf}$ for a ϵ_s^f in Eq. 20, $(U_{\ell 0})_{osf}$ can be determined for a given U_{g0} for each particle employed. Figure 8 shows the comparison between the calculated and experimental values of $(U_{\ell 0})_{osf}$. The average coefficient of variation is 8%.

Height of the Packed Section, H'_{pa}

The height of the packed section in the semifluidized bed can also be measured directly by visualization. From a material balance for the solid particles, the height of the packed section in the semifluidized bed can be expressed by

$$H'_{pa} = \frac{W_s/(\rho_s A) - H_c \epsilon_s'^f}{\epsilon_s'^p - \epsilon_s'^f} \tag{29}$$

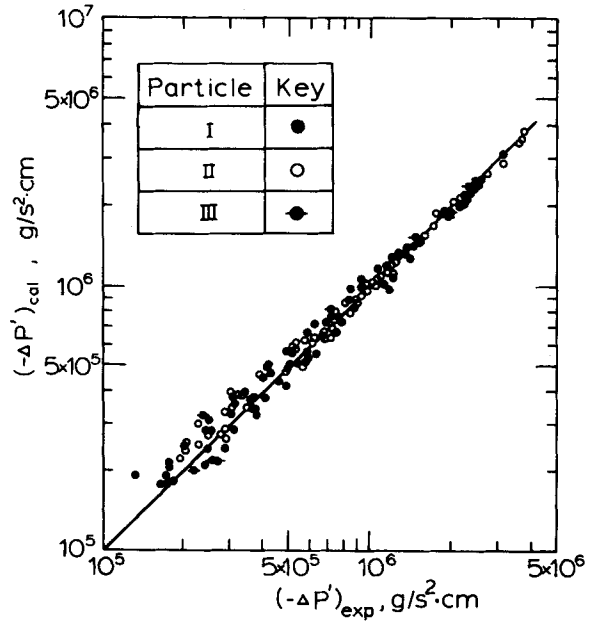

Figure 10. Comparison of the calculated and experimental values of $(-\Delta P')$ in the semifluidized bed.

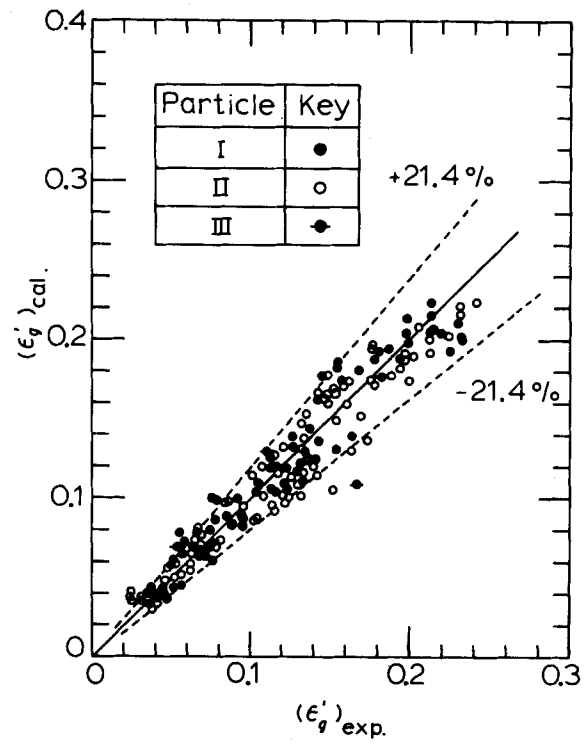

Figure 11. Comparison of the calculated and experimental values of ϵ'_g in the semifluidized bed.

where $\epsilon_s'^f$ is the solids holdup in the fluidized section, which can be approximated by the solids holdup in the fully fluidized bed under the same operating conditions. $\epsilon_s'^p$ is the solids holdup in the packed section, which is assumed to be 0.6. For a given $U_{\ell 0}$, U_{g0}, and W_s, $\epsilon_s'^f$ can be obtained by the equations described before for each particle employed in this study. Thus H'_{pa} can be calculated by Eq. 29 for each given H_c.

Figure 9 shows the comparison between the calculated and experimental H'_{pa}. The average coefficient of variation is 14.3%.

Pressure Drop

The pressure drop in the semifluidized bed can be considered as the sum of the pressure drop in the packed section $(-\Delta P')^p$, and that in the fluidized section, $(-\Delta P')^f$, that is,

$$(-\Delta P') = (-\Delta P')^p + (-\Delta P')^f \tag{30}$$

$(-\Delta P')^p$ can be estimated by multiplying the pressure gradient of the packed bed calculated from Eq. 9 by the height of the packed section, while $(-\Delta P')^f$ can be calculated from Eq. 16 by substituting $(H_c - H'_{pa})$ for H. The comparison of the pressure drop in the semifluidized bed predicted and obtained experimentally is shown in Figure 10. It is seen that the agreement is good.

Gas Holdup

The average gas holdup in the semifluidized bed can be expressed by

$$\epsilon'_g = \left(\frac{H'_{pa}}{H_c}\right)\epsilon_g'^p + \left(1 - \frac{H'_{pa}}{H_c}\right)\epsilon_g'^f \tag{31}$$

Figure 11 shows the comparison between the gas holdups calculated from Eq. 31 and those experimentally obtained. The average coefficient of variation is 21.4%.

ACKNOWLEDGMENT

The work was supported by the National Science Foundation Grant No. CPE 7921068.

NOTATION

A = cross-sectional area of testing column, cm^2
D = diameter of testing column, cm
D_e = equivalent diameter, defined by Eq. 12, cm
d_p = equivalent diameter of particle, cm
f = modified friction factor, defined by Eq. 11
g = gravitational acceleration, cm/s^2
H = height of bed expansion, cm
H_c = distance between the upper and lower retaining grids in the testing column, cm
H'_{pa} = height of packed section in the semifluidized bed, cm
k = ratio of the volume of the wake region to that of the bubble region $(\epsilon^f_w/\epsilon^f_g)$
n = Richardson-Zaki index
$\left(-\frac{dP}{dz}\right)$ = pressure gradient, $g/s^2 \cdot cm^2$
$(-\Delta P)$ = static pressure drop, $g/s^2 \cdot cm$
Re = liquid Reynolds number, defined by Eq. 14
U_{g0} = superficial gas velocity, cm/s
U_i = extrapolated superficial liquid velocity in the liquid-solid fluidized bed as the bed voidage approaches 1, cm/s
$U_{\ell 0}$ = superficial liquid velocity, cm/s
U_0 = velocity due to buoyancy, defined by Eq. 22 or 24, cm/s
$\overline{U}_\ell$ = linear liquid velocity, cm/s
W_s = initial weight of solid particles, g
x = ratio of solids holdup in the wake region to that in the liquid-solid fluidized bed region $(\epsilon_{sw}/\epsilon_{sf})$

Greek Letters

α = coefficient defined by Eq. 23 or 25
ϵ = holdup
ϵ''_g = gas holdup in the two-phase bubble column system
ϵ_{sf} = solids holdup in the liquid-solid fluidized region
ϵ_{sw} = solids holdup in the wake region
θ = holdup based on the gas-liquid phases
ρ = density, g/cm^3
ϕ_s = sphericity

Superscripts

$'$ = semifluidized bed
p = packed bed
f = fluidized bed
$\ell - s$ = liquid-solid
$\ell - g$ = liquid-gas
$g - \ell$ = gas-liquid

Subscripts

cal = calculated
exp = experimental
f = friction
g = gas phase
ℓ = liquid phase
osf = onset semifluidization
s = solid phase
w = wake region

LITERATURE CITED

Armstrong, E. R., C. G. J. Baker, and M. A. Bergougnou, "The Effects of Solids Wettability on the Characteristics of Three Phase Fluidization," *Fluidiz. Tech.* **1**, p. 405 (1976).

Babu Rao, K., and L. K. Doraiswamy, "Combined Reactors: Formulation of Criteria and Operation of a Mixed Tubular Semifluidized Reactors," *AIChE J.*, **16**, p. 273 (1970).

Baker, C. G. J., S. D. Kim, and M. A. Bergougnou, "Wake Characteristics of Three-Phase Fluidized Beds," *Powder Technol.*, **18**, p. 201 (1977).

Bhatia, V. K., and N. Epstein, "Three-Phase Fluidization: A Generalized Wake Model," *Proc. Int. Symp. on Fluidization and its Applications*, Cepadues-Editions, Toulouse, p. 380 (1974).

Chementator, "Fluidized-Bed Ion Exchange Systems are Available," *Chem. Eng.* (July 24, 1972).

Chern, S.-H., K. Muroyama, and L.-S. Fan, "Hydrodynamics of Constrained Inverse Fluidization and Semifluidization in a Gas-Liquid-Solid System," paper 65a, 74th AIChE Annual Meeting, New Orleans, LA (1981); *Chem. Eng. Sci.* **38**, p. 1167 (1983).

Darton, R. C., and D. Harrison, "Gas and Liquid Hold-up in Three-Phase Fluidization," *Chem. Eng. Sci.*, **30**, p. 581 (1975).

Efremov, G. I., and I. A. Vakrushev, "A Study of the Hydrodynamics of Three-Phase Fluidized Beds," *Int. Chem. Eng.*, **10**, p. 37 (1970).

El-Temtamy, S. A., and N. Epstein, "Bubble Wake Solid Content in Three-Phase Fluidized Beds," *Int. J. Multiphase Flow*, **4**, p. 19 (1978).

Fan, L. T., and C. Y. Wen, "Semifluidization: Mass Transfer in Semifluidized Beds," *AIChE J.*, **5**, p. 407 (1959).

Fan, L. T., and C. Y. Wen, "Mechanics of Semifluidization of Single Size Particles in Solid-Liquid Systems," *AIChE J.*, **7**, p. 606 (1961).

Fan, L. T., and E. H. Hsu, "Semifluidized Bed, Historical Perspective and Future Prospective," Seminar on Theoretical and Industrial Aspects of Semifluidization and Fluidization, Rourkela, India (Nov. 28–30, 1978).

Fan, L.-S., K. Muroyama, and S.-H. Chern, "Hydrodynamic Characteristics of Inverse Fluidization in Liquid-Solid and Gas-Liquid-Solid Systems," *Chem. Eng. J.*, **24**, p. 143 (1982).

Matsuura, A., T. Akehata, and T. Shirai, "Friction Factor of Gas-Liquid Cocurrent Downflow through Packed Beds," *Kagaku Kogaku Ronbunshu*, **3**, p. 122 (1977).

Muroyama, K., K. Hashimoto, T. Kawabata, and M. Shiota, "Axial Liquid Mixing in Three-Phase Fluidized Beds," *Kagaku Kogaku Ronbunshu*, **4**, p. 622 (1978).

Nicklin, D. J., "Two Phase Bubble Flow," *Chem. Eng. Sci.*, **17**, p. 693 (1962).

Ostergaard, K., *Studies of Gas-Liquid Fluidization*, Danish Technical Press, Copenhagen (1969).

Richardson, J. F., and W. N. Zaki, "Sedimentation and Fluidization: Part I," *Trans. Inst. Chem. Eng.*, **32**, p. 35 (1954).

Rigby, G. R., and C. E. Capes, "Bed Expansion and Bubble Wakes in Three-Phase Fluidization," *Can. J. Chem. Eng.*, **48**, p. 343 (1970).

Roy, G. K., and P. S. Gupta, "Prediction of the Packed Bed Height in a Gas-Solid Semifluidization," *Ind. Eng. Chem. Process Des. Develop.*, **13**, p. 219 (1974).

Roy, G. K., and H. N. Sharat Chandra, "Liquid-Solid Semifluidization of Heterogeneous Mixtures, II: Prediction of the Minimum Semifluidization Velocity," *Chem. Eng. J.*, **12**, 77 (1976).

Roy, G. K., and K. J. R. Sarma, "Prediction of Pressure Drop Across a Liquid-Solid Semifluidized Bed," *Indian J. of Tech.*, **16**, p. 89 (1978).

Sato, Y., T. Hirose, and T. Ida, "Upward Cocurrent Gas-Liquid Flow in Packed Beds," *Kagaku Kogaku*, **38**, p. 534 (1974).

Turpin, J. L., and R. L. Huntington, "Prediction of Pressure Drop for Two-Phase, Two-Component Cocurrent Flow in Packed Beds," *AIChE J.*, **13**, p. 1196 (1967).

Wallis, G. B., *One-dimensional Two-phase Flow*, McGraw-Hill, Inc. (1969).

Wen, C. Y., S. C. Wang, and L. T. Fan, "Semifluidization in Solid-Gas Systems," *AIChE J.*, **9**, p. 317 (1963).

Manuscript received June 24, 1982; revision received March 10, and accepted May 19, 1983.